

PAPER • OPEN ACCESS

## X-ray spectral analysis of surface structures formed on copper alloys during film fasting

To cite this article: V I Kubich *et al* 2021 *J. Phys.: Conf. Ser.* **1901** 012091

View the [article online](#) for updates and enhancements.



The banner features a decorative top border with a repeating pattern of red, white, and blue diagonal stripes. On the left, the ECS logo is displayed in green and blue, followed by the text 'The Electrochemical Society' and 'Advancing solid state & electrochemical science & technology'. To the right of this text is a logo for the 18th International Meeting of the Solid State Ionics Society (IMCS18). The main text of the banner reads '239th ECS Meeting with IMCS18', 'DIGITAL MEETING • May 30-June 3, 2021', and 'Live events daily • Free to register'. On the right side, there is a graphic showing a person's head with a glowing blue brain and network lines, and a laptop icon. A red button with white text 'Register now!' is positioned at the bottom right of the banner.

**ECS** The Electrochemical Society  
Advancing solid state & electrochemical science & technology

**239th ECS Meeting with IMCS18**

DIGITAL MEETING • May 30-June 3, 2021

Live events daily • Free to register

**Register now!**

# X-ray spectral analysis of surface structures formed on copper alloys during film fasting

V I Kubich<sup>1</sup>, O G Cherneta<sup>2</sup>, V M Yurov<sup>3\*</sup> and V S Oleshko<sup>4</sup>

<sup>1</sup>National University "Zaporizhzhya polytechnic", Zaporizhia, Ukraine

<sup>2</sup>Dniprovsk State technical university, Kamenskoye, Ukraine

<sup>3</sup>Karaganda University E.A. Buketova, st. Universitetskaya, 28, Karaganda 100028, Kazakhstan

<sup>4</sup>Moscow Aviation Institute (National Research University), Moscow, Russia

[ovs\\_mai@mail.ru](mailto:ovs_mai@mail.ru), [ocherneta@gmail.com](mailto:ocherneta@gmail.com), [schmirung@gmail.com](mailto:schmirung@gmail.com)

**Abstract.** The paper establishes the nature of the redistribution of chemical elements and their concentration in secondary surface structures for the material systems "steel 45XN2MFA-grease-BrOTsS4-4-2.5", "steel 45XN2MFA-grease-BrOTsS4-4-4", "steel 45XN2MFA-grease-L-63", tested under the conditions of simulating film starvation when lubricated with 15W40 Lukoil-Super SAE SG/CD engine oil. Since the formula obtained by us includes the Gibbs energy, the self-organization of the structure under consideration naturally also enters. General laws of self-organization are observed when a number of conditions are met: irreversibility, openness (nonequilibrium), nonlinearity, instability (coherence), dissipativity. All these elements were observed and described by us in this work. It is due to self-organization that the distribution of chemical elements carbon and oxygen occurred on the surfaces L63 and BrOF4-4-4. To this effect must be added a decrease in the surface tension of the lubricant.

**Keywords:** tribosystem of materials, chemical element, copper alloy, surface, scanning area, analysis.

## 1. Introduction

Disclosure of the mechanisms for reducing friction and wear in tribological couplings of mechanical engineering objects on the basis of the established patterns of formation of tribological and secondary structures in the near-surface layers underlies not only increasing their operational reliability, but also seems to be a toolkit in developing measures to ensure the manifestation of self-organization processes in tribosystems of materials. Such processes include, for example, selective transfer. It is especially important to take into account when, in complex tribosystems of materials working with the supply of lubricant, hidden, previously unrevealed and undescribed interaction mechanisms may appear under certain conditions. The kinematics and dynamics of such mechanisms are primarily determined by the motion and forces of interaction between the components of the lubricating medium and alloying elements of alloys when changing modes of power, high-speed loading and lubrication. The components of the lubricating medium and alloying elements of the alloy represent a complex environment, however, the calculations do not take into account the compressibility of the lubricating fluid, the dependence of its viscosity characteristics on pressure and temperature. A micropolar fluid is characterized by three physical constants  $\mu$ ,  $\alpha$ ,  $\gamma$ , in contrast to a Newtonian fluid, which has only one constant  $\mu$  - viscosity. The parameter  $\alpha$  has the dimension of viscosity. Since it manifests itself as a result of taking into account microrotations, it is called the coefficient of viscosity during rotational motion (coefficient of vortex viscosity). It characterizes the resistance to rotational movement, just as the coefficient  $\mu$  characterizes the resistance to translational movement. The  $\gamma$  coefficient has the



dimension [ $\ell^2$ ] [ $\mu$ ], and with its help the length parameter  $\ell = \sqrt{\gamma/4\mu}$  is determined, which characterizes the size of the lubricating liquid microparticles.

Such tribosystems of materials are used, for example, in plain bearings, where the functions of the trunnion are performed by alloyed steels and cast irons. The role of the sleeve is performed either by inserts with an antifriction layer, or by a one-piece sleeve made of a copper alloy, polymer, powder composite material, etc., and their use in mechanical engineering objects is very wide. Based on the above, the need for further disclosure of previously identified and development of new mechanisms of contact interaction between surface secondary structures is determined, and the development of recommendations for their implementation. It is also obvious that the mechanisms must be disclosed taking into account the mass transfer between the chemical elements of tribosystem materials. It is also obvious that the availability of data on the molar masses of lubricants, patterns of change in the ratios of their surface tension and viscosity coefficients when using commercial additives, such as remetalizers, geomodifiers, will indicate the peculiarities of the behavior of the lubricating layers in tribo-conjugations. Moreover, we should talk about both the circulating lubricant in the tribological system, and about the structures that are orderly formed and connected with each other and directly with the materials of the contacting surfaces. The issues of studying the properties of new antifriction materials, including those for plain bearings, are currently relevant, as evidenced by a very long series of scientific publications, including those of the authors of [1-4].

Thus, in [1], the secondary structures on the friction surfaces of aluminum alloys were investigated, the difference between the secondary structures from the surface of the alloys to friction was analyzed, and the properties of the AO-6.1 aluminum alloy proposed by the authors with the BrO8S12 bronze were compared. Aluminum antifriction alloys, yielding to bronzes in mechanical properties, significantly surpass them in tribological ones. Aluminum alloys wear out the steel counterbody 6 times less than bronze; the scuffing load of aluminum alloys is 2.5 times greater than the scuffing load of bronze; the wear rate of aluminum alloys is 2 times less than the wear rate of bronze. The paper does not disclose the mechanism for reducing friction, but only shows the ability of an aluminum antifriction alloy to self-organize with the formation of beneficial secondary structures on the friction surface, which became one of the determining factors when choosing it as a material for monometallic bearings of diesel locomotive turbochargers. Individual zones of friction surfaces are not analyzed. In [2], a deep analysis of metal antifriction materials (babbitts B88, B83, B16, BKA, BK2,  $SnSb_8Cu_4$ ) was carried out and technological recommendations were developed for plasma-powder surfacing of a babbitt alloy of the  $SnSb_8Cu_4$  brand on a steel base St3sp. Tribotechnical tests of the developed new babbitt were carried out under conditions of dry sliding friction. At the same time, attention was not paid to the peculiarities of the formation of surface structures; to a greater extent, the wear resistance of the deposited metal was evaluated, depending on the volume structure. In [3], the scientific foundations of technologies for the formation of new functional-gradient layered compositions and coatings from composite materials based on aluminum, tin and their alloys with enhanced tribotechnical properties were developed. The author found that the wear of composite materials occurs predominantly by the oxidative mechanism; matrix alloys have a high adhesive wear component. The following systems are considered as composite materials:  $Al-Si-Mg$ ,  $Al-Si-Cu$ ,  $Al-Mg$ ,  $Al-Cu-Mg$ ,  $Al-Sn-Cu$ ,  $Sn-Sb-Cu$ , containing micron-sized particles of silicon carbide ( $SiC$ ), titanium carbide ( $TiC$ ), aluminum oxide ( $Al_2O_3$ ), intermetallic compounds of the  $A_xTi_y$  system, silvery graphite ( $C$ ), as well as submicron particles of boron ( $B$ ), boron carbide ( $B_4C$ ), carbon nanotubes and powders of modified shungite rock. As a result of contact interaction on the friction surfaces of the samples of the developed composite materials, a transition layer or "third body" is formed, which, according to the results of X-ray phase analysis, is a mechanical mixture of the materials of the test sample, counterbody and their oxides. In [4], it is proposed to obtain a combined electroerosive coating on bronze BrOCS5-5-5 alloyed with silver, lead, copper, which allows the formation of running-in structures on its surface, which reduce friction force by 20% during the running-in period. Such a coating is not a continuous (homogeneous) layer, but is in the form of discrete zones with a maximum thickness of 30  $\mu m$ , that is, a regular surface microrelief is formed. In this case, the resulting bronze

bushings have high reliability and durability during operation due to the fact that even with the destruction of the coating, the bearing continues to work [4]. However, the question is not given to the disclosure of the mechanism of manifestation of the friction reduction system. The work [5] presents the results of tribotechnical tests of new experimental graphitized steels, secondary aluminum alloys AL<sub>25</sub>, AlSi<sub>12</sub>Cu<sub>1</sub>(Fe), ASCh-2 cast iron, copper alloys BrOTsS4-4-4, BrOTsS4-4-2.5, L63 in collaboration with steel 45HN2MF on small-sized samples according to the friction pattern "movable disk - fixed block".

This was part of the research aimed at developing recommendations for the selection of materials for the plain bearing of a turbocharger of an internal combustion engine. Moreover, in contrast to the works [1-4], the loading modes were simulated, causing the violation of the lubrication conditions when working in the environment of 15W40 Lukoil-Super engine oil. Discontinuity of lubrication during lubrication of a bearing occurs during operation of a turbocharger, and it is important to ensure stable lubrication of the friction surfaces to improve the reliability of the plain bearing and the turbocharger as a whole. The lack of stability of the lubricating action of the boundary films during film starvation was shown by BrOCS4-4-2.5, ASCh-2, and some graphitized steels. Greater stability of the lubricating layers was caused by BrOCS4-4-4, L63, graphitized steel (*C* – 1.78%, *Si* – 2.25%, *Cu* – 3.19%, *Al* – 0.23%, *Mn* – 0.64, *Ni* – 0.15%, *Cr* – 0.17%, *S* – 0.016%, *P* – 0.029%). The formed lubricating formations ensured boundary friction without the external features of catastrophic destruction for  $6.5 \pm 0.5$  min at a load of 165 N. At a load of 250 N for 3 min, the lubricating layers did not completely collapse. Also, only when testing L63 was the fact of the formation of a secondary lubricant of a dark color in the aggregate state of a paste of a sticky consistency with a content of elements: *C* – 0.55%, *O* – 0.85%, *Fe* – 4.43%, *Cu* – 66.5% was revealed, *Zn* – 27.66%. Such a composition withstood a load of 350N for 2.5 minutes, then its continuity on the friction surface was broken. It seems obvious that the stability of the manifestation of the lubricating action under the given modes is determined by the composition of the interacting structures. However, there is no information on the chemical composition of the surface structures of the isolated materials in [5], which necessitates their X-ray spectral analysis.

In work [7] it is emphasized that in modern operating conditions of lubricated tribosystems one of the most promising is the fluid friction mode, which is realized in plain bearings and significantly reduces the power loss to overcome friction. And in this lubrication mode, the undoubted advantage belongs to the hydrodynamic process, in which the lubricating medium plays the leading role - one of the main structural elements of plain bearings. It is also emphasized there that information on the chemical composition of the surface structures of liquid lubricants, structural elements made of an alloy on the bearing surface, shows that the main performance characteristics of the bearings under consideration depend on the viscosity parameter.

However, as we have shown in [8], the surface tension plays a certain role on the distribution of chemical impurities in lubricating structures.

The aim of the work is to establish the nature of the redistribution of chemical elements and their concentration in secondary surface structures for the material systems "steel 45XN2MFA-grease-BrOTsS4-4-2.5", "steel 45XN2MFA-grease-BrOTsS4-4-4", "steel 45XN2MFA- grease-L-63" tested under the conditions of simulating film starvation when lubricated with 15W40 Lukoil-Super SAE SG/CD engine oil. This assumes a physical assessment of possible cases of behavior of the lubricant when changing its parameters: change in dispersion due to abrasion of the surface of the materials of the friction pair; changing the adhesion of carbon and oxygen due to surface tension; change in temperature and pressure in the lubricating medium, due to changes in its viscosity; a change in the chemical  $\mu$  and electrical potential  $\phi$ , leading to oxidative processes with the participation of oxygen.

## 2. Objects and methods of research

For research, we used the working surfaces of the block specimens, Figure 1, made of BrOTsS4-4-2.5, BrOTsS4-4-4 rectangular bronzes and L63 cylindrical brass and their transverse thin sections. The subject of research was the chemical composition of secondary microstructures formed in the near-

surface layers of the pads in contact with a rotating disc made of 45KhN2MFA steel. The tribological state of the surfaces of copper alloys was formed at sliding friction  $V = 0.78$  m/s and normal step loading of 165 N, 250N, 350N for 3 min on the residual components of the mineral motor oil 15W40 Lukoil-Super SAE SG/CD [5]. At the same time, on the surface of the samples, the following were separately visualized: on L63 brass a golden zone with a reddish tint and a dark zone; dark and yellow zones on bronzes. These zones are a kind of markers for the manifestation of types of lubrication within the nominal friction area of the pads. Based on the characteristic colors and residual lubricating formations, the following assumption is made. In the golden zone, dry friction occurred with discontinuity of the formed lubricating formations, i.e. film starvation with respect to the formed secondary lubricant. In the dark zone, there was boundary boundary lubrication with the solid phase material, i.e. film starvation relative to the action of the components of the original lubricant (motor oil). In the yellow zone, boundary friction (boundary lubrication) took place without disrupting the continuity of the lubricant, i.e. in the absence of film starvation. Thus, the yellow and dark zones can be considered as initial (basic) ones for assessing the nature of the distribution of chemical elements in the formed secondary surface structures.

X-ray spectral analysis of the surface and transverse sections of the pads was carried out on a REMMA JSM-6360 LA setup in the mode of linear probe displacement  $U = 15$  kW,  $I = 50$  nA. The penetration depth of the X-ray beam into the analyzed layers for chemical elements was:  $h_c \approx 2.2$   $\mu\text{m}$ ;  $h_{Fe, Sn} \approx 0.7$   $\mu\text{m}$ ;  $h_{Cu} \approx 0.6$   $\mu\text{m}$ ,  $h_{pb} \approx 0.5$   $\mu\text{m}$ . The chemical composition, the concentration of elements were determined by zones (points). The distribution of scanning zones (points) was dictated by the need to obtain the most complete picture of the layer-by-layer and local character of the distribution of chemical elements.

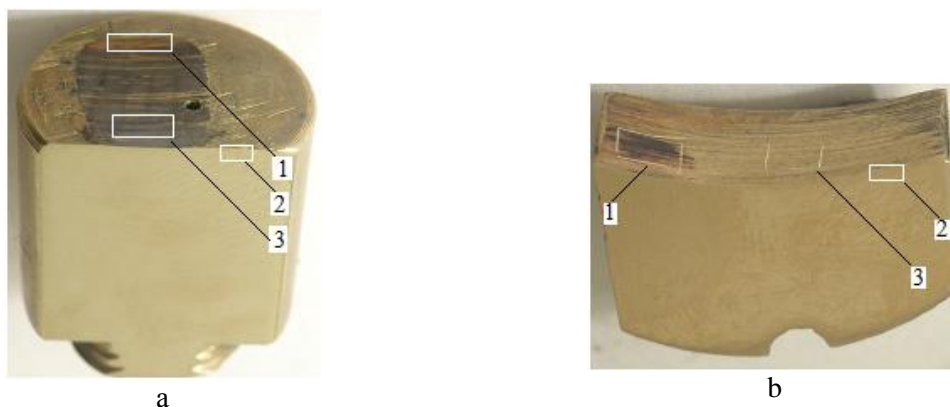


**Figure 1.** Samples-pads of copper alloys: a – brass L63; b – bronze BrOTS4-4-2.5; BrOCS4-4-4; 1, 2, 3 – scan zones

### 3. Results of the experiments and discussion

Figure 1-10 shows photographs of working surfaces and thin sections, and tables 1-8 show the distribution of chemical elements by zones obtained as a result of their scanning. In general, the following is noted. First, on the working surfaces (zone A for A63, zone B for BrOCS4-4-4, BrOCS4-4-2.5) during film starvation at a depth of 0.6-2.2  $\mu\text{m}$ , structures are formed in the form of mechanical mixtures of chemical elements of copper alloys and alloying elements from steel 45KhN2MFA. At the same time, the exit from the steel due to the weakening of bonds in the crystal lattice and the concentration on the surface of the copper alloy due to the adhesive component is more characteristic of such elements as *Fe* and *Cr*. The formed structures contain oxide inclusions. This is indicated by the presence of oxygen, and to a greater extent for bronzes - 0.6-0.8%, to a lesser extent for brass - 0.4-0.6%. Adsorption is also noted in a small amount of 0.6-1.4% from engine oil, while in smaller concentrated volumes of surface structures, the proportion of carbon increases to 0.9-1.6%.

No significant changes in the chemical composition of copper alloys are observed along the transverse section during film starvation at a depth of up to 10  $\mu\text{m}$ . The number and distribution of chemical elements is statistically average equal to the distribution in the underlying layers, i.e. in the total volume of the material. There is no capillary saturation of the surfaces with the degradation products of engine oil, which is indicated by the absence of carbon, sulfur in a depth of 0  $\mu\text{m}$  to 5  $\mu\text{m}$ . Moreover, the structures L63 and BrOCS4-4-4 are dense, without deformation flows of metal and distorted macro-texture. The exception is bronze BrOTs4-4-4, for which the surface at a depth of 15 microns has deformation pores with carbon. The texture of the cross section is distorted at a depth of 190 microns. This indicates the dominant influence of the adhesive interaction of the secondary structures of BrOCS4-4-4 with 45XH2MFA with very high activity.

Secondly, the state of surfaces formed during boundary lubrication is also characterized by the presence of transferred Fe and Cr, oxide compounds, and carbon. However, their ratio has a significant difference. So, for L63 with boundary lubrication on a secondary lubricant on the iron surface, it is 1.7 times more than with film starvation. For BrOCS4-4-2.5, the amount of iron in the surface structure during film starvation is 6 times higher than its amount with boundary lubrication. At the same time, iron does not concentrate at all on the surface of BrOCS4-4-2.5 with boundary lubrication, only carbon in a small amount (up to 0.93%) in the absence of oxides. Analysis of the given data for alloy L63 showed the following, Fig. 2-4, table 1.2.

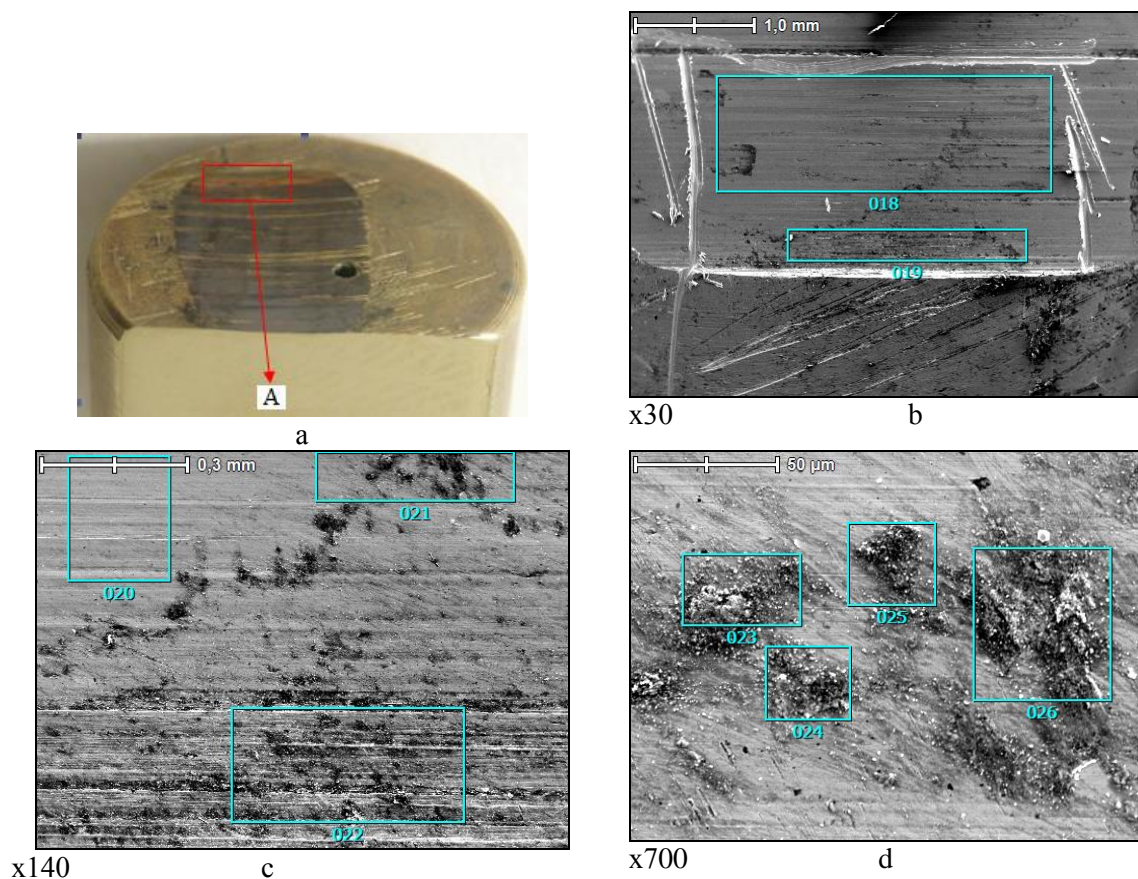


**Figure 2.** Working surface of material L63: A – golden zone with a reddish tint; a – general view; c,d – photographs of the surface and separate scanning areas with a distinctive microprofile

The characteristic features of the surface in zone A are:

– areas with a smoothed relief 2x2 mm in size within the analyzed depths of up to 0.5 microns, there is an increase in the% copper content by 1.15 times compared to its volumetric content. Moreover, the same decrease in the % content is characteristic of zinc. The smoothed relief indicates a dense packing of the structure of thin surface layers and their inherent properties to resist shear with a very small fraction of the adhesive friction component. The presence of oxygen may indicate the oxidative wear mechanism of the analyzed area;

– areas with a size of 0.3x0.3 mm with a porous ruled relief and areas of 30x30  $\mu\text{m}$  with a porous point relief within the analyzed depths up to 0.5  $\mu\text{m}$  there is an increase in the% copper content by 1.12 times compared with its volumetric content. At the same time, zinc becomes 2.6 times less. Apparently, zinc in very small local volumes dissolved and went into the lubricating medium, and its mass content was replaced by *Fe* ( $\approx 3.6\%$ ), *Cr* ( $\approx 7.2\%$ ), *Al* ( $\approx 0.9\%$ ), *Si* ( $\approx 0.33\%$ ) as a result of mechanochemical interaction with steel and *C* ( $\approx 2.2\%$ ) with *S* ( $\approx 0.6\%$ ) as a result of their adsorption and adhesion from the secondary lubricant, Table 1 of zone 023-026. The described relief with the average statistical redistribution of chemical elements indicates the appearance of an increased fraction of the adhesive interaction of local microfragments of surface structures with the active zones of steel, i.e. grasping. The latter, due to the increased proportion of oxygen by 1.8 times in comparison with the smoothed areas, excludes the manifestation of the mechanism of plasticization and smoothing. In this case, the formed oxides are harder than within the smoothed areas.

**Table 1.** Distribution of chemical elements by scanning areas of zone A of material L63

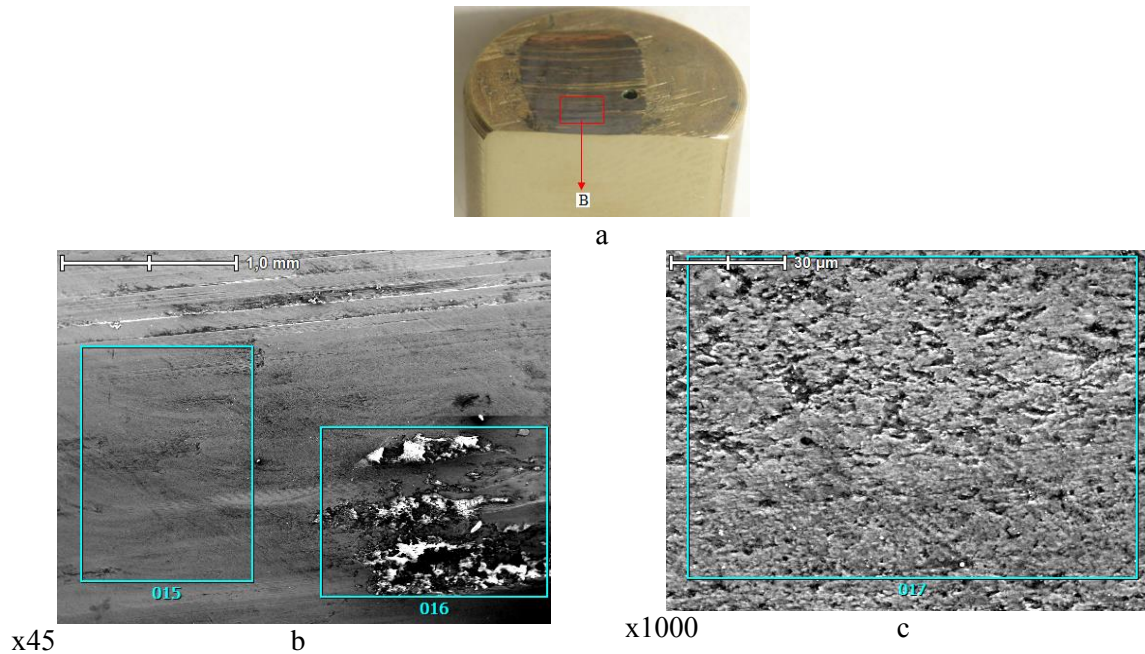
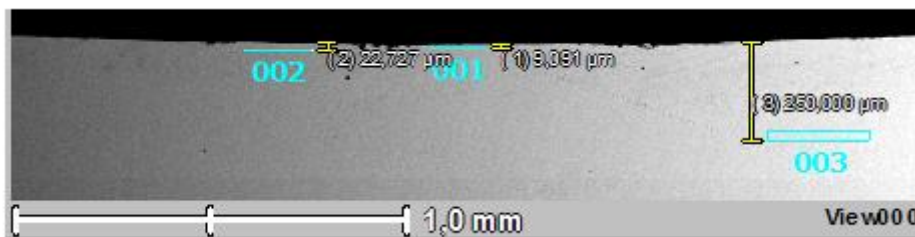
Zone No.	Concentration of chemical elements, %								
	<i>C</i>	<i>O</i>	<i>Al</i>	<i>Si</i>	<i>S</i>	<i>Cr</i>	<i>Fe</i>	<i>Cu</i>	<i>Zn</i>
018	0.67	0.41	-	-	-	-	2.11	75.82	21
019	1.13	0.67	-	-	-	1.98	2.16	66.32	27.73
020	-	-	-	-	-	-	1.64	82.1	16.26
021	1.13	0.15	-	-	-	2.55	2.13	81.19	12.85
022	1.29	0.69	-	-	-	2.98	1.94	64.41	28.69
023	0.98	0.57	0.71	0.18	0.53	7.75	2.34	78.16	8.78
024	0.9	0.9	0.64	0.32	0.06	7.71	3.75	74.04	11.67
025	2.29	0.53	0.25	0.47	-	6.15	2.67	73.82	13.82
026	2.35	1.09	1.3	0.37	0.67	-	5.44	70.46	18.33

A characteristic feature of the surface in zone B is a smoothed profile, which, with a magnification of x1000, represents uniformly distributed fine-pored (cellular) structures with a size of 10x10 microns. The exception is minor foci of damage to such a microprofile in areas of 0.6x1 mm. There is no obvious decrease in the% copper content. In this case, zinc is partially replaced by transferred iron up to 4% and chromium up to 1.4%, and the dark background is due to adsorbed relatively uniformly distributed carbon up to 1% from the secondary lubricant.

The described picture of the redistribution of chemical elements in the formed structures during film starvation caused, according to the data of [5], an abrupt change in the friction coefficient from 0.2 to 0.15 and to 0.2 within three minutes at loads of 250-350  $\mu\text{m}$  with a subsequent increase in the friction coefficient to 0.4 at 450 N. And with a decrease in the load to 165 N, a decrease in the coefficient of friction to 0.28. From the above, it seems obvious that such secondary structures can partially resist pathological damage in the indicated field of force loading for 3 minutes. Taking into account the calculated thicknesses of the boundary lubricating layers considered in [6], which are 0.4-4 microns at small radii of single surface irregularities up to 13 microns, within the analyzed thickness of the L63 surface 0.5-2.2 microns when switching to the mode film starvation, the following can be assumed. Favorable conditions are created for the formation of adhesive bonds of oil components with active metal centers with low values of shear strength. This, in turn, can be considered as one of the rationales in the recommendation of the material L63 for a turbocharger sleeve bearing with an operating range of 90,000-100,000  $\text{min}^{-1}$ .

**Table 2.** Distribution of chemical elements by scanning areas of zone B of material L63

Zone No.	Concentration of chemical elements, %					
	<i>C</i>	<i>O</i>	<i>Cr</i>	<i>Fe</i>	<i>Cu</i>	<i>Zn</i>
015	1.45	1.06	-	3.76	65.54	28.21
016	2.97	0.47	1.43	4.28	60.38	30.48
017	0.55	0.85	-	4.43	66.5	27.66

**Figure 3.** Working surface of material L63; B – dark zone; a – general view; b, c – photographs of the surface and separate scanning zones with a distinctive micro-profile**Figure 4.** Surface of a transverse section of material L63, x55: zone 001 (Cu 65.16%; Zn 34.84%); zone 002 (Cu 60.26%; Zn 39.74%); zone 003 (Cu 64.82%; Zn 35.18%);

The analysis of the given data on the BrOCS4-4-2.5 alloy showed the following, Fig. 5-7, table 3-5. The characteristic features of the surface in zone A (Fig. 5 b, c) are strip-like areas formed in the direction of sliding without obvious pathological differences. The relief feature is that the bottom of the stripes is smoother than the tops. A change in the content of copper and alloying elements in bronze with boundary lubrication is practically not observed, with the exception of certain areas in which there is an insignificant transfer of chromium up to 2.6% and iron up to 1.5% with a very small amount of oxygen up to 0.4%, Table 3.

Characteristic features of the surface in zone C (Fig. 6 b, c) are areas up to 6-8 mm wide with a smoothed and “rippled, loose” strip-like relief. The stripes of the sections are formed in the direction of



sliding and alternate aperiodically with each other. Within the analyzed depths of up to 0.5 microns, there is a slight decrease in the% copper content by 10-13 % times in comparison with its volumetric content. At the same time, the same decrease in the% content is characteristic of zinc, tin and lead. There is a fairly high average statistical content of transferred iron 8-14% and chromium 1.6-2.2 (Table 4). At the same time, these alloying elements of steel can be both pure and in the form of oxides, since there is an insignificant presence of oxygen of 0.6-0.94%. No carbon was found on the surface from the composition of the engine oil, which excludes the possibility of the formation of a solid lubricating secondary material, as is typical for the A63 alloy.

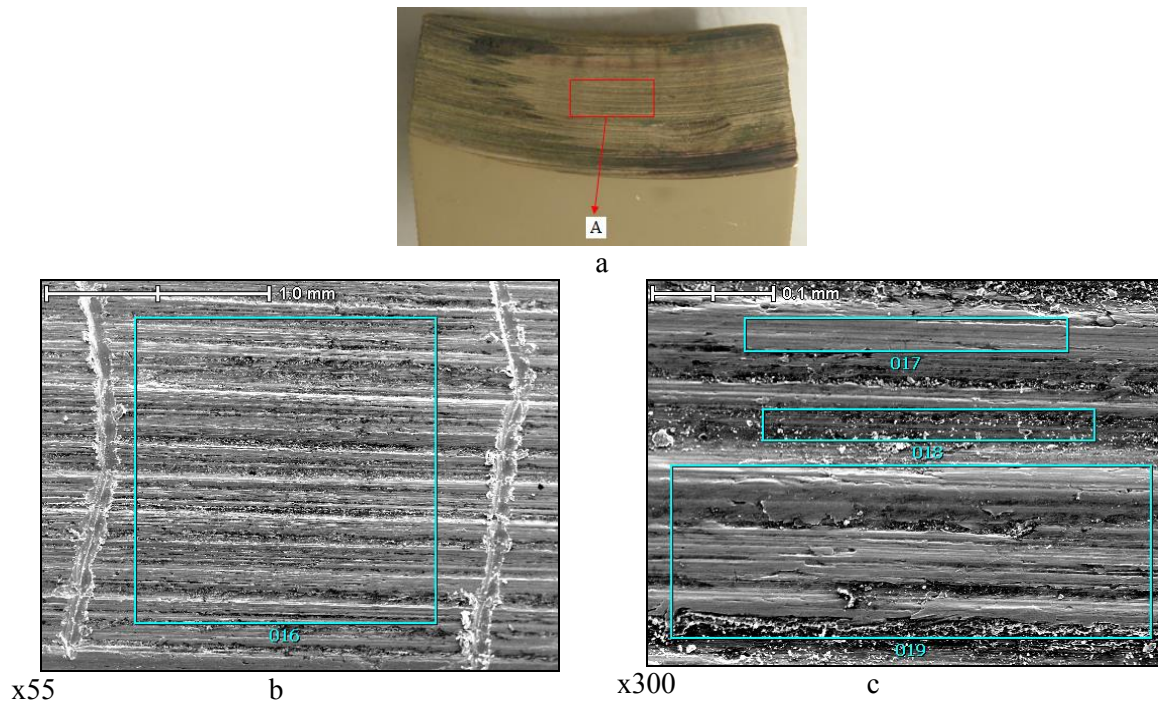


**Figure 5.** Working surface of BrOTsS4-4-2.5 material: A – yellow zone; a – general view; b, c – photographs of the surface and separate scanning zones with a distinctive micro-profile

**Table 3.** Distribution of chemical elements by scanning areas of zone A of the BrOCS4-4-2.5 material

Zone No.	Concentration of chemical elements, %						
	<i>O</i>	<i>Cr</i>	<i>Fe</i>	<i>Cu</i>	<i>Pb</i>	<i>Sn</i>	<i>Zn</i>
016	-	2.02	0.92	87.17	3.11	3.74	3.04
017	-	-	-	90.5	2.1	3.93	3.48
018	0.41	2.67	1.52	85.93	4.25	3.42	1.81
019	-	1.32	-	89.39	3.79	3.52	1.98

It seems obvious that there is a significant difference in the amount of transferred iron Fe during film starvation. Its increase is 4-7 times compared to mass transfer with boundary lubrication. This fact determines the lack of stability of the model tribo-conjugation with bronze BrOTsS4-4-2.5 noted in [5]. In this regard, it is not advisable to consider recommendations for using this material to initiate self-organizing processes under conditions of film starvation with low friction and wear indicators.

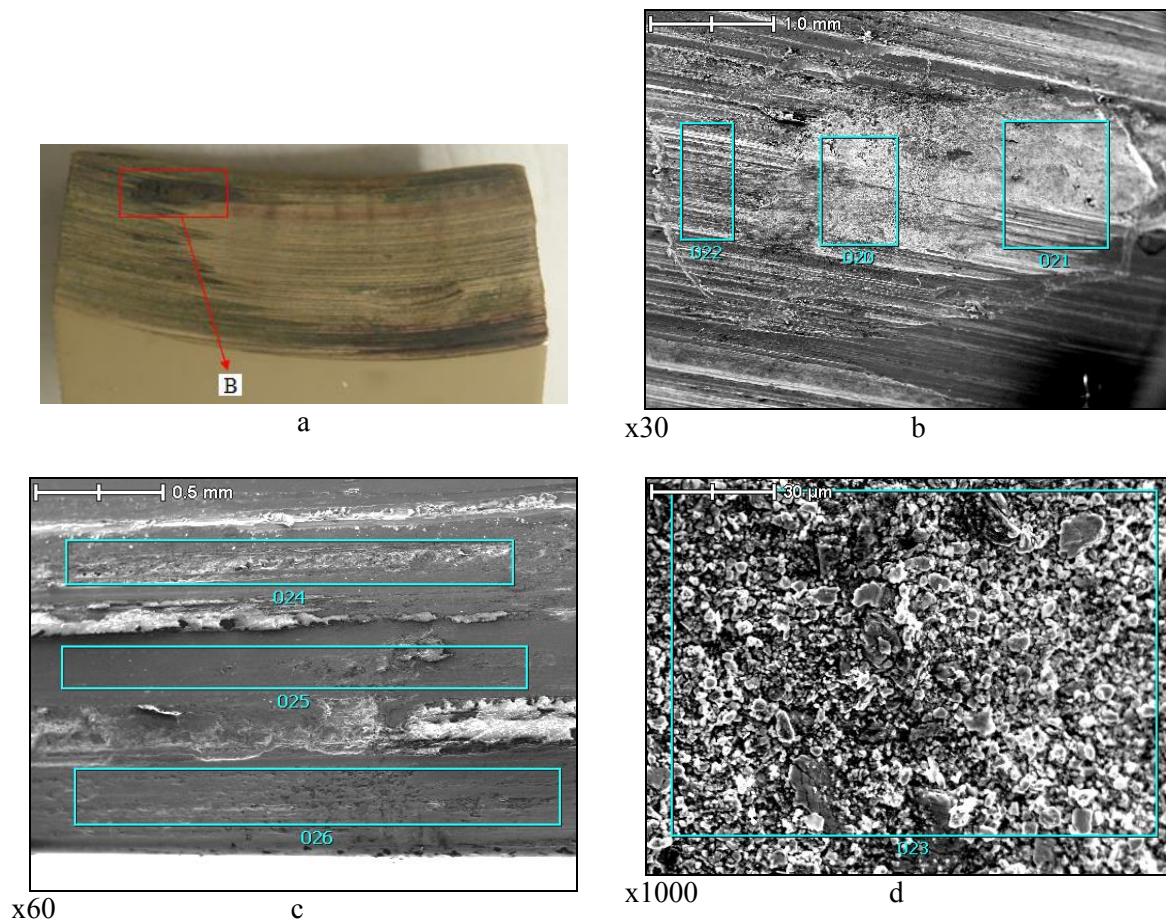


**Figure 6.** Working surface of the BrOTsS4-4-2.5 material: V – dark zone; a – general view; b, d – photographs of the surface and individual scan areas with a distinctive microprofile

**Table 4.** Distribution of chemical elements by scanning areas of zone B of BrOCS4-4-2.5 material

Zone No.	Concentration of chemical elements, %								
	<i>O</i>	<i>Cr</i>	<i>Fe</i>	<i>Cu</i>	<i>Pb</i>	<i>Sn</i>	<i>Zn</i>	<i>Al</i>	<i>Si</i>
020	0.94	2.12	15.08	78.85	1.06	3.42	0.53	-	-
021	0.44	2.65	12.00	76.47	2.27	3.06	2.12	-	-
022	0.89	1.91	8.44	82.55	1.85	3.30	1.07	-	-
024	0.8	4.96	6.39	83.01	1.7	2.41	-	0.33	0.44
025	0.62	-	9.09	86.72	1.31	2.26	-	-	-
026	0.84	1.28	9.56	83.9	2.39	2.04	-	-	-
028	0.93	1.78	14.84	77.41	1.65	3.42	-	-	-

The analysis of the given data on the BrOTsS4-4-4 alloy showed the following, Figure 8-10, Table 6-8. The characteristic features of the surface in zone A (Fig. 8) is a flat, flat profile without any foci of pathological destruction. Moreover, the distribution of chemical elements over the surface is even, practically not differing from the average distribution in the volume of the material. There is a presence of carbon adsorbed from engine oil up to 1%. In this case, there is no oxygen. The characteristic features of the surface in zone B (Fig. 9) is also a flat, flat profile with a slight formation of pores of various depths, rounded and elongated. At the same time, the distribution of chemical elements over the surface is even, but with a 1.8 times reduced zinc content. Moreover, the amount of

adsorbed carbon increased 1.8 times and oxygen was added with the transferred iron up to 3%, Table 7. Alternatively, carbon displaced zinc by mass formation of the secondary structure, which went into the engine oil during tests. The cause of pore formation is most likely in the transferred gland. However, its amount is at least 2.6-4.6 times less than it was for BrOCS4-4-2.5.

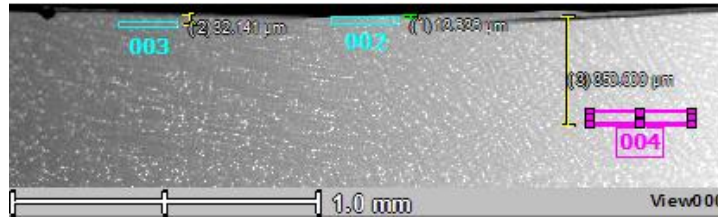


**Figure 7.** The surface of the transverse section of the material BrOTsS4-4-2.5; x55

**Table 5.** Distribution of chemical elements over the scanning areas of the transverse section of the BrOCS4-4-2.5 material

Zone No.	Concentration of chemical elements, %			
	<i>Cu</i>	<i>Zn</i>	<i>Sn</i>	<i>Pb</i>
002	92.30	2.17	3.54	2.00
003	91.62	3.42	3.89	1.06
004	92.58	2.98	3.41	1.03

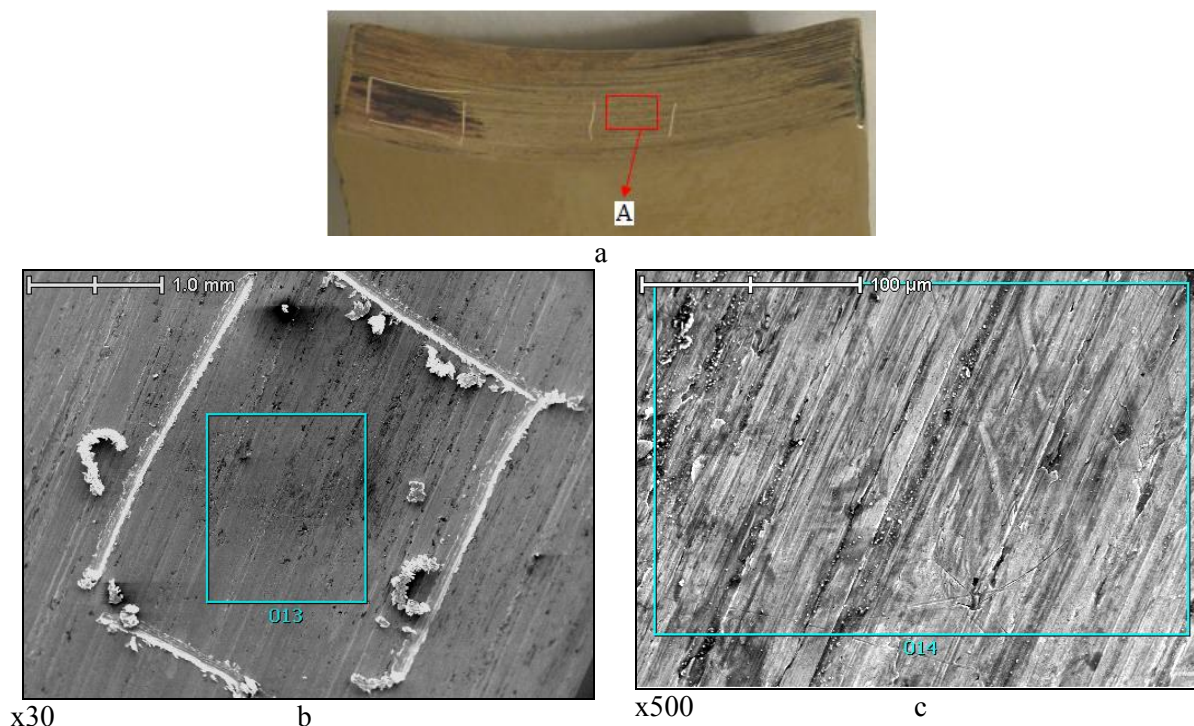


**Figure 8.** Working surface of the BrOTsS4-4-4 material: A – yellow zone; a – general view; b, c – photographs of the surface and separate scanning zones with a distinctive micro-profile

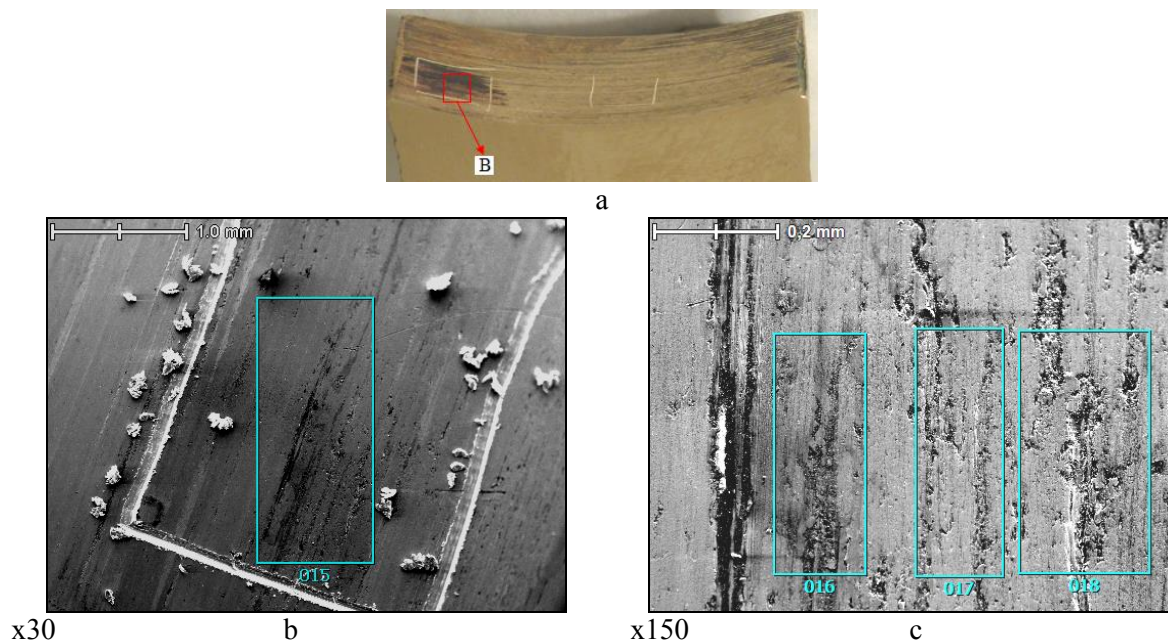
Based on the above, it seems obvious that the described redistribution of chemical elements, taking into account their mass transfer and adsorption, determines the stability of the functionality of the lubricating layers, including during film starvation. BrOCS4-4-4 is capable of creating the preconditions for carbon adsorption and thereby providing the ability to work for a short time during film starvation, which was obtained earlier in [5]. Thus, as in the case of L63, favorable conditions for the formation of adhesive bonds of oil components with active metal centers with low values of shear strength appear. This, in turn, can be considered as one of the rationales in the recommendation of the material for the BrOCS4-4-4 sliding bearing of a turbocharger with an operating range of 90,000-100,000  $\text{min}^{-1}$  [6].

**Table 6.** Distribution of chemical elements by scanning areas zone A of material BrOTsS4-4-4

Zone No.	Concentration of chemical elements, %				
	<i>C</i>	<i>Cu</i>	<i>Zn</i>	<i>Sn</i>	<i>Pb</i>
013	0.93	88.43	3.31	4.02	3.32
014	0.65	88.04	4.34	4.27	2.7

**Table 7.** Distribution of chemical elements by scanning areas zones B of material BrOTsS4-4-4

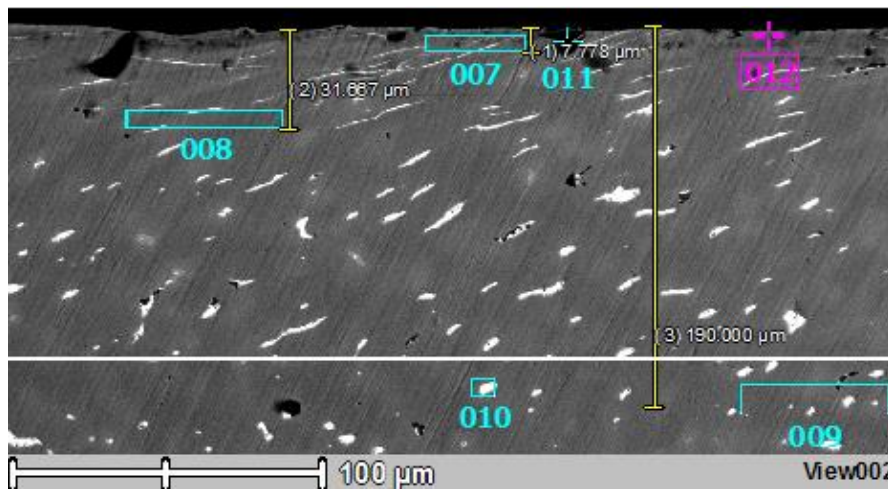
Zone No.	Concentration of chemical elements, %						
	<i>C</i>	<i>O</i>	<i>Fe</i>	<i>Cu</i>	<i>Zn</i>	<i>Sn</i>	<i>Pb</i>
015	1.46	0.9	2.79	87.33	1.93	3.37	2.21
016	1.39	0.97	2.85	85.52	2.06	4.35	2.87
017	1.58	0.53	2.9	86.03	1.59	4.51	2.87
018	1.43	0.78	3.66	83.6	2.95	4.38	3.19



**Figure 9.** Working surface of BrOCS4-4-4 material: V – dark zone; a – general view; b, c – photographs of the surface and separate scanning zones with a distinctive micro-profile

**Table 8.** Distribution of chemical elements by scanning areas zones B of material BrOTsS4-4-4

Zone No.	Concentration of chemical elements, %						
	<i>C</i>	<i>O</i>	<i>Fe</i>	<i>Cu</i>	<i>Zn</i>	<i>Sn</i>	<i>Pb</i>
015	1.46	0.9	2.79	87.33	1.93	3.37	2.21
016	1.39	0.97	2.85	85.52	2.06	4.35	2.87
017	1.58	0.53	2.9	86.03	1.59	4.51	2.87
018	1.43	0.78	3.66	83.6	2.95	4.38	3.19

**Figure 10.** The surface of the transverse section of the BrOTsS4-4-4 material; x450**Table 9.** Distribution of chemical elements by scanning areas of the transverse thin section of the BrOCS4-4-4 material

Zone No.	Concentration of chemical elements, %				
	<i>C</i>	<i>Cu</i>	<i>Zn</i>	<i>Sn</i>	<i>Pb</i>
007	-	89.86	3.34	4.30	2.49
008	-	93.26	1.84	3.62	1.27
009	-	92.38	1.39	4.21	2.02
010	-	76.42	2.37	5.26	15.94
011	28.52	67.06	-	2.29	2.13
012	3.45	92.04	2.06	2.45	-

The above X-ray data can be regarded as manifestations of nanosuspensions arising from the rotation of bearings. The theory of effective viscosity of rarefied coarsely dispersed suspensions was developed by A. Einstein. He found that the effective viscosity coefficient  $\eta$  increases in proportion to the volume concentration  $\varphi$  of dispersed particles:

$$\eta(\varphi) = \eta_0(1 + 2.5\varphi). \quad (1)$$

where  $\eta_0$  is the coefficient of viscosity of the carrier fluid.

In deriving this relation, the perturbations introduced into the velocity field of the carrier fluid by an isolated solid particle were taken into account, and the additional stresses associated with this were calculated. Subsequent experiments showed that formula (1) is valid only for  $\varphi \leq 10^{-3}$ . The conclusion

that the effective viscosity of a nanofluid depends not only on the volume concentration of nanoparticles, but also on their mass and size, is one of the key ones in [9]. It was found that the dependence of the viscosity coefficient on the volume concentration of nanoparticles is described by a quadratic function of the form (2), unless these concentrations are too high.

$$\eta(\varphi) = \eta_0(1 + k_1(\mathbf{R}, \mathbf{M})\varphi + k_2(\mathbf{R}, \mathbf{M})\varphi^2). \quad (2)$$

The coefficients of this correlation are functions of both the sizes of nanoparticles  $\mathbf{R}$  and their masses  $\mathbf{M}$ . An important criterion that determines the growth of the effective viscosity of a nanofluid is the ratio of the mass densities of the material of nanoparticles and molecules  $\rho = \rho_n / \rho_m$ .

The transparency in the coefficients  $k_1$  and  $k_2$  can be clarified using the approach outlined by us in [8]. For the viscosity coefficient it is possible to write (see formula (4) from work [8]):

$$\eta = \tilde{N} \cdot \frac{\sigma \cdot \rho}{G^0}, \quad (3)$$

where  $\sigma$  is the surface tension of the lubricant,  $\rho$  is the density of the lubricant,  $G^0$  is the Gibbs energy of the lubricant, and  $C$  is some constant.

The change in the Gibbs energy  $dG^0$  due to physicochemical processes that occur, for example, during the rotation of bearings, is equal to:

$$dG^0 = -SdT + VdP + \sigma dS + \sum_i \mu_i dn_i + \varphi dq \quad (4)$$

This equation expresses the increment of the Gibbs energy of the system in terms of the algebraic sum of the increments of other types of energy. This sum indicates five possible processes of transformation of surface energy (respectively, from left to right): 1) into Gibbs energy  $dG$ ; 2) to heat  $-SdT$ ; 3) into mechanical energy  $VdP$ ; 4) into chemical energy  $\sum \mu_i dn_i$ ; 5) into electrical energy  $\varphi dq$ . This demonstrates broader possibilities for achieving a minimum energy and corresponds to certain surface phenomena, for example, (following the scheme from left to right) such as 1) a change in reactivity with a change in dispersion, 2) adhesion and wetting, 3) capillarity, 4) adsorption, 5) electrical phenomena. Thus, equations (3) and (4) cover all cases of the behavior of the lubricant when its parameters change:

- a change in dispersity due to abrasion of the surface of materials of a friction pair;
- a change in the adhesion of carbon and oxygen due to surface tension;
- changes in temperature and pressure in the lubricating medium, leading to a change in its viscosity;
- a change in the chemical  $\mu$  and electric potential  $\varphi$ , leading to oxidative processes with the participation of oxygen. Since formula (3) includes the Gibbs energy, the self-organization of the structure under consideration naturally also enters. General laws of self-organization are observed when a number of conditions are met: irreversibility, openness (nonequilibrium), nonlinearity, instability (coherence), dissipativity [9]. All these elements were observed and described by us above. It is due to self-organization that the distribution of chemical elements carbon and oxygen occurred on the surfaces L63 and BrOF4-4-4. To this effect it is necessary to add a decrease in the surface tension of the lubricant.

#### 4. Conclusion

The performed X-ray spectral analysis of the surfaces of copper-containing materials made it possible, on the basis of the kinetics of chemical elements, to present the characteristic features of the surface structures of copper alloys, which determine the manifestation of mechanisms for reducing friction in the previously tested model tribo-couplings of sliding. The experimental data considered by us allow us to draw a conclusion about the self-organization of surface structures during film starvation. In this case, the manifestation of irreversibility lies in the fact that during the operation of the material, both in its surface and in the inner layers, certain qualitative changes occur, confirmed by X-ray spectral analysis, which, under certain conditions, lead to wear, chipping or volumetric destruction, forming micro- and macro relief. The manifestation of openness (non-equilibrium) lies in the fact that friction is not constant and depends on certain tribological phenomena that occur in the lubricating film

between sliding bodies. The manifestation of nonlinearity arises in the power-law model of contact, which takes into account the gaps caused by micro- and macro-relief, the number of actual and contour contact areas in the loading zone, contact stiffness, as well as the normal and tangential force acting on local interaction areas, contact angle. The manifestation of instability (coherence) is characterized by the Rayleigh-Taylor instability. The manifestation of dissipativity is outlined by the proportionality of energy dissipation per one rotation cycle in the simulated slip tribo-conjugation. The presented expressions for the viscosity coefficient and the Gibbs energy increment indicate that during the transition to film starvation, all possible cases of the behavior of the lubricant with a change in its parameters are possible, which determine the formation of surface self-organizing structures in copper alloys.

## 5. References

- [1] Mirovov A E, Aytyukhyy G G and Gershman E I 2020 *Bulletin of VNIIZhT*. **79** No 4 217
- [2] Gurkin S V, Kobernik N V and Mikheev R S 2018 *Welding production* No 4 43
- [3] Mikheev R S, Kobernik N V and Kalashnikov I E 2020 *Metally* No.5 99
- [4] Tarelnik V B, Antoshevsky B V, Martsinkovsky V S, Karp P A and Dzyuba A V 2015 *Bulletin of KhNTUSG im. P. Vasilenka*. **159** 90
- [5] Kubich V I and Klimin V V 2015 *Problems of rubbing and communication* **1**(66) 54
- [6] Kubich V I, Zadorozhnaya E A and Cherneta O G 2020 *Lecture Notes in Mech. Eng.* 1137
- [7] Mukutadze M A 2012 *Vestnik RGUPS* **1**(45) 196
- [8] Kubich V I and Yurov V M 2016 *Problems of grating and communication* **1**(70) 58
- [9] Rudyak V Ya and Lezhnev E V 2015 *Doklady AN VSh RF* No 3(28) 99

## 6. Acknowledgement

The work was carried out under the program of the Ministry of Education and Science of the Republic of Kazakhstan Grants No. 0118RK000063 and No. F.0780.